

Metaorder modelling and identification from public data

Ezra Goliath^a, Tim Gebbie^a

^a*Department of Statistical Science, University of Cape Town, Rondebosch 7701, South Africa*

Abstract

Market-order flow in financial markets exhibits long-range correlations. This is a widely known stylised fact of financial markets. A popular hypothesis for this stylised fact comes from the Lillo–Mike–Farmer (LMF) order-splitting theory. However, quantitative tests of this theory have historically relied on proprietary datasets with trader identifiers, limiting reproducibility and cross-market validation. We show that the LMF theory can be validated using publicly available Johannesburg Stock Exchange (JSE) data by leveraging recently developed methods for reconstructing synthetic metaorders. We demonstrate the validation using 3 years of Transaction and Quote Data (TAQ) for the largest 100 stocks on the JSE when assuming that there are either $N=50$ or $N=150$ effective traders managing metaorders in the market.

Keywords: LMF theory, metaorders, order-splitting, long-memory, auto-correlation function, power-law

Subject Areas: Econophysics, financial markets, agent-based modeling, electronic trading.

1. Introduction

Long-range autocorrelations (LRC) of market-order flow is a widely known macroscopic phenomenon of financial markets [12, 13]. The idea is that macroscopic phenomena in continuously traded double-auction intraday financial markets are predominantly due to the aggregated effects of microscopic actions *i.e.* the bottom-up aggregation of individual trades. This can be contrasted both with top-down causes such as market wide information shocks, or the coordinated actions of agents at the macro-economic level [20] and prices that result for Walrusian like closing auctions.

One hypothesis is that LRC arise in the market-order flow due to the order-splitting behaviour of traders [13]. The key microscopic contributor is then the aggregation of metaorders after they have been broken up and mixed in real markets. Even if the reason (or the cause) for the metaorders themselves is top-down from market actors operator at lower frequency at the level of mutual funds and macro-economic events. This top-down cause can be thought to come from some latent order-book [18].

This idea then links the microscopic properties of trades directly to macroscopic averaged measurables; the trade-sign auto-correlations and the shape of the price impact. Such a direct link should be surprising if one places more value on exogenous information shocks, fundamental information, and general news flow, and then some sort of idea of predictability in stock market price changes themselves, rather than endogenous causes of dynamics and emergence.

Concretely, it was proposed that the decay exponent γ of the autocorrelation function (ACF) of the trade signs (say ϵ) are directly related to the power-law exponent α of the probability of finding a metaorder of length L through the relation: $\gamma = \alpha - 1$ [13].

This result is known as the LMF theory¹ and was initially argued via simulation, but was later empirically validated on the Tokyo Stock Exchange (TSE) [16, 17].

This validation is a remarkable and surprising result! The importance of this result has been discussed elsewhere [11, 3], but essentially it is a phenomenological law that explains the convexity of the price impact and hence the square-root law of the price impact of metaorders. It also supports a very specific microscopic cause for the key macroscopic universal features of intraday stock market dynamics and how the order-flow can be predictable even when the price changes are not.

Verification of the LMF theory on other markets following Sato and Kanazawa [16] has proven to be difficult because of the need to acquire datasets that contain trader identification information and broker codes. These fields are required to be able to reconstruct the underlying metaorders from the market transaction and limit order update messages. Here a metaorder is a linked sequence of buy (or sell) orders $+1(-1)$ coming from a single agent operating in the market. There are then many such agents and hence many metaorders. We label the metaorders with index j to refer to the j -th metaorder $Q^{(j)}$ comprising of n orders $q_i^{(j)}$ for $i \in [1 : n]$. A metaorder could be considered to represent the simplest type of trading schedule.

¹That the probability of metaorders of length L is $P(L) \propto L^{-\alpha-1}$ for $\alpha > 1$, and the autocorrelations in the trade signs ϵ are $C(\tau) \propto \tau^{-\gamma}$ for a delay τ such that $\gamma = \alpha - 1$.

Email addresses: g1tezr001@myuct.ac.za (Ezra Goliath), tim.gebbie@uct.ac.za (Tim Gebbie)

The details of the parent order generating the metaorders are typically considered to be private and hence not made more generally available to researchers and market participants.

However, recent work on metaorder reconstruction using very simple distributional assumptions has proved to have been able to preserve key aggregate properties of financial markets [14]. Here we combined these two innovations to address the data issue and reverse engineer the individual trades to generate synthetic metaorders from publicly available Johannesburg Stock Exchange (JSE) data for the largest 100 stocks (Table 4). This was carried out over a three year period, from 1 January 2023 to 31 December 2025 using trade by trade event data (See Appendix 7.1). The data includes only publicly available trades and order-book updates, and was sourced through the BMLL Data Lab platform [2].

In Section 2 we provide details about the data source and how the data was pre-processed. In Section 3 we describe how we have implemented the method of Maitrier et al. [14], and then provide some of the missing algorithm details [10]. We explicitly provide two simple variants of the metaorder reconstruction method, and demonstrate how we have validated the metaorders.

In Section 4 we validate the Lillo-Mike-Farmer theory [13] following the broad idea of Sato and Kanazawa [16] but with the reconstructed metaorders following our implementation of the method of Maitrier et al. [14]. Part of the metaorder reconstruction method requires choosing the number of effective traders operating within the market, here for indicative purposes we choose: $N = 50$, and $N = 150$. The other part is making distributional assumptions about the metaorder themselves. The results are reasonably robust to a reasonable choice of both the number of traders and the distributional shape.

We then provide a brief conclusion in Section 5. The key result is that we have evidence of the Lillo et al. [13] theory holding on the JSE despite using reconstructed orders. This suggest the metaorder recovery methods are reasonably robust in the volume regime that the LMF theory holds.

2. Data Description

The analyses are based on high-frequency Level 1 trade data, which provides the basic information for each executed trade, including the timestamp, traded price, traded volume, and trade direction (± 1 for buy and sell respectively). Cleaning and some pre-processing was done beforehand. Specifically, the mid-prices just before and just after the trades were included in the data sets.

The data extended from 1 January 2023 to 31 December 2025 for the assets in Table 4 (See Section 7.1). Using the data, we were able to calculate the intraday volatility, daily volume, and mid-prices. This processed data was then used to generate the synthetic metaorders. Table 5

in Section 7.2 has an example snippet of the data that was used.

To generate synthetic metaorders, we applied Algorithm 1, which assigns trades to synthetic traders using a mapping function that preserves the chronological order of trades. This procedure requires specifying N the number of synthetic traders, and the distribution of their trader participation, here either homogeneous or power-law. Using this "mapping", sequences of consecutive trades with the same sign for each synthetic trader are defined as metaorders and compiled using Algorithm 2. Table 6 in Section 7.3 has an example snippet of the output from Algorithm 2.

These metaorders are subsequently used to study the square-root law of metaorder impact, the time independence of metaorder impact, the execution profile and the post execution profile.

3. Generating synthetic metaorders

Numerous attempts have been made to generate synthetic metaorders from public data. The validity and quality of these synthetic metaorders is tested by comparing their reproduced stylised facts to empirically proven stylised facts of metaorders. These stylised facts are [14]:

1. The *square root law* (SQL) of metaorder impact,
2. The *time independence* of metaorder impact,
3. The *concave profile* of metaorder execution, and
4. The *post execution decay* of metaorder impact.

The validation of these stylised facts are individually addressed in sections 3.2, 3.3, 3.4 and 3.5 below. First, we will discuss the metaorder generating algorithm of Maitrier et al. [14] in Section 3.1.

3.1. The metaorder generating algorithms

Previous attempts have failed to reproduce all the stylised facts of metaorders. As far as we know, the only method that can generate metaorders which reproduce all stylised facts is the one proposed in [14]. Their algorithm uses a mapping function to assign trades to a predetermined number of traders while maintaining chronological order of the the trades.

We have used both homogeneous: $f \equiv f_0$, and power-law: $P(f) \propto f^{-\delta}$, distributions for our trader participation distributions. The homogeneous distribution was defined such that $f_1 = f_2 = \dots = f_N$. Samples from the power-law were obtained using inverse transform sampling. Our implementation of this algorithm allows us to specify a minimum and maximum number of trades that a trader can have, and the power-law exponent δ . We have set default values of minimum = 1, maximum = total number of trades for the day and $\delta = 2$.

Algorithm 1 Mapping Function

Require: Number of traders N and trader participation distribution F

Ensure: Trades are assigned according to participation weights p_j for the j -th trader:

- 1: Draw $f_j \sim F$ for $j = 1, \dots, N$
- 2: Normalise frequencies:

$$p_j = \frac{f_j}{\sum_k f_k}$$

- 3: Compute cumulative probabilities

$$c_j = \sum_{k=1}^j p_k$$

with $c_0 = 0$

- 4: **for** each order q_i in the market **do**
 - 5: Draw a random variable $U \sim \mathcal{U}(0, 1)$
 - 6: Find the trader j such that $c_{j-1} \leq U < c_j$
 - 7: Assign the trade to j -th agent.
 - 8: **end for**
-

Algorithm 2 generates the synthetic metaorders from public TAQ data. The assignment of trades to specific traders is controlled by Algorithm 1. It is critically important that trades remain in chronological order and that the mapping is unique. Once a trade is assigned to a trader, it cannot be assigned to a different trader as well. This corresponds to sampling without repetition [14].

In real markets, trader activity distributions are well approximated by power-laws [14]. However, the precise distribution and the optimal number of traders N to generate the synthetic metaorders are not known a priori. To account for this uncertainty, we generate metaorders using both homogeneous and power-law trader participation distributions, as well as multiple values of N . This gives us a crude understanding of how the different trader participation distributions and different N values affect the quality of the metaorders.

3.2. The Square Root Law

Given the j -th metaorder made up of n_j trades, we define the total executed volume of the metaorder as:

$$Q^{(j)} = \sum_{i=1}^{n_j} q_i^{(j)}. \quad (1)$$

where $q_i^{(j)}$ is the volume of the i -th trade of metaorder j . The measured price impact of the metaorder is computed from change in the limit-order book induced by the transactions resulting from the metaorder and measured by the change in the mid-price from the start to the end of the metaorder:

$$I(Q^{(j)}) = \epsilon^{(j)} \times \left(\ln(m_{n_j+1}^{(j)}) - \ln(m_0^{(j)}) \right). \quad (2)$$

Algorithm 2 Generation of Synthetic Metaorders

Require: Cleaned public trade data for a given asset and trading day: trade volumes q_ℓ and m_ℓ mid-prices at order book events $\ell \in [1, L]$.

Ensure: Set of synthetic metaorders: $\{q_i^{(j)}\}_{i=1}^{n_j}$.

- 1: Compute daily traded volume: $\ell \in [1, L]$:

$$V_D = \sum_{\ell=1}^L q_\ell$$

- 2: Compute the intraday volatility:

$$\sigma_D = \frac{m_{\max} - m_{\min}}{m_{\text{open}}},$$

using the maximum: m_{\max} , minimum: m_{\min} , and first mid-price: m_{open} , of the day.

- 3: Apply the Mapping Function (Algorithm 1) to assign each trade to a synthetic trader while maintaining chronological order.
 - 4: Sort trades by trader and timestamp
 - 5: Define the j -th metaorder as a sequence of trades with the same trade sign (from the same trader): $\{q_i^{(j)}\}_{i=1}^{n_j}$
 - 6: Compute features of metaorder:
 - 6.1 log mid-prices just before: $\ln(m_0^{(j)})$,
 - 6.2 number of child orders: n_j
 - 6.3 log mid-prices just after: $\ln(m_{n_j+1}^{(j)})$
 - 6.4 total traded volume of the metaorder: $Q^{(j)}$
 - 6.5 execution duration: T_j
 - 6.6 any other relevant quantities.
 - 7: Aggregate metaorder statistics
 - 8: Only return those with more than 1 child order
-

Here m_{n_j+1} is the mid-price just after the metaorder ends, m_0 is the mid-price just before the metaorder starts and ϵ is the trade sign of the metaorder where $j \in [1, N]$, for the N traders to index the trade schedule from Equation 1.

The SQL states that the price change induced by a large metaorder of volume Q is proportional to \sqrt{Q} [14]. The theoretical price impact of metaorders is given as:

$$I(Q) = Y \sigma_D \sqrt{\frac{Q}{V_D}}, \quad (3)$$

where Q is the total volume traded in the metaorder, V_D is the daily traded volume, σ_D is the intraday volatility² and Y is a prefactor [19]. Here for notational convenience we have dropped the metaorder and trader label; this is implicit in its definition.

Figure 1 is a log-log plot of metaorder impact for two stocks (Figure 1a) and for the top 100 stocks (Figure 1b)

²We used a 20 day moving average for both V_D and σ_D

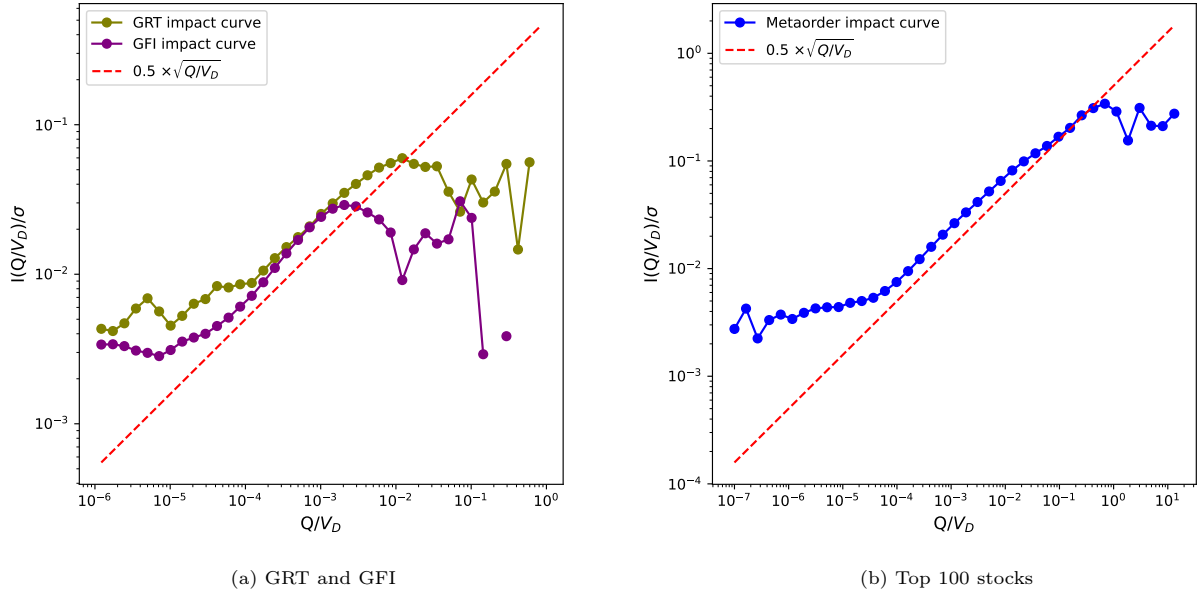


Figure 1: SQL for (a) GRT and GFI displayed individually and (b) all the stocks in the top 100 stocks compiled into a single line with the theoretical SQL given in red. In both cases a homogeneous distribution was used for the trader participation with the number of traders set to 4.

with the theoretical SQL given in red. Metaorders were generated by specifying 4 traders and a homogeneous trader participation distribution³. The figure was created by first binning by Q/V_D into 40 equally spaced bins in the logarithmic space and then taking the bin centers as the x domain values. The range, y value for each bin was then taken to be the the average metaorder impact of the observations in that bin.

Figure 1a shows the metaorder impact for GFI (a more liquid stock) and GRT (a less liquid stock). From this figure it is clear that the impact curve for GRT lies above the impact curve for GFI. This indicates that for an equal relative order size Q/V_D , the metaorder impact of GRT is larger than for GFI. This is a consequence of lower liquidity in GRT. Despite this, for $Q/V_D \in [10^{-3.5}, 10^{-1.5}]$ we see that GRT obeys the SQL and for $Q/V_D \in [10^{-5}, 10^{-2.5}]$ GFI obeys the SQL. Values outside of these approximate intervals are noise relative to the hypothesis with smaller trades exceeding the SQL fit and larger trades having lower impact than the fitted SQL.

Figure 1b shows the metaorder impact curve for all stocks in the top 100 compiled into a single curve by doing the binning procedure for all stocks together instead of separately. From this figure it is clear that the overall metaorder impact of the top 100 stocks obeys the SQL for $Q/V_D \in [10^{-4}, 10^{0.5}]$ when normalised for the different intraday volatilities⁴. We again see divergence from the

theoretical SQL outside of this range but this is again due to noise.

3.3. Time independence of metaorder impact

It has been shown that metaorder impact is independent of metaorder duration T [14].

Figure 2 shows the independence of metaorder impact with respect to T for GFI and GRT. A histogram of the metaorder durations is given in grey and the normalised impact is overlayed. Metaorders were once again generated by specifying 4 traders and a homogeneous trader participation distribution. The x axis is logarithmically scaled.

Given the logarithmically scaled x axis, it is clear that the impact remains relatively flat as T increases. This indicates approximate independence between the impact and T . Both subfigures show long left tails with short right tails, indicating far more metaorders with short T 's compared to long T 's. Figure 2a specifically has a fatter tail than Figure 2b which could be indicative of more algorithmic and high frequency trading occuring for GFI.

3.4. The concave profile of metaorder impact

So far we have only investigated the impact of entire metaorders, now we investigate the impact of individual trades inside each metaorder. An analysis of 400 000 metaorders showed that there are two stages of metaorder

³The mapping function requires us to specify the number of traders and trader distribution apriori. Check Section 3.1 for details on the mapping function and metaorder generating algorithm.

⁴This suggests two different normalisation procedures, first by

relative volatility, the other, using the ADV to shift the price impact.

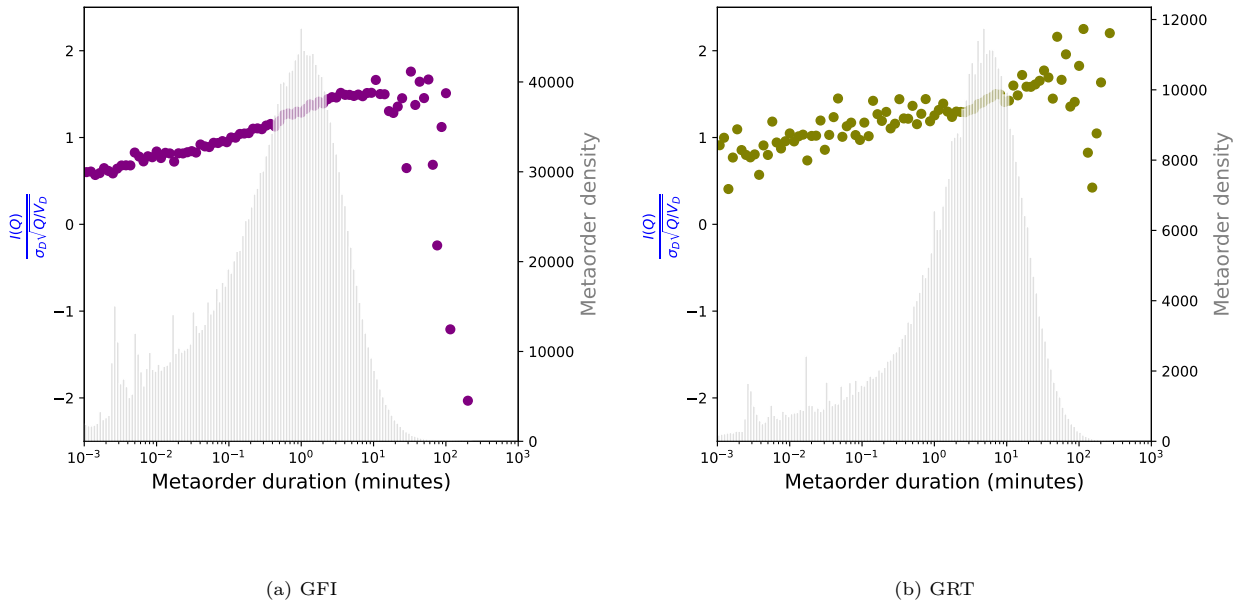


Figure 2: Approximate independence of metaorder impact with respect to the duration of the metaorder for (a) GFI (more liquid) and (b) GRT (less liquid). Majority of metaorders have a duration between 1 and 30 minutes.

impact, the concave profile during execution and the convex decay after execution [1]. For now we will investigate the concave profile during metaorder execution.

We take the theoretical price impact profile during metaorder execution to be:

$$I(\phi \times Q) = \sqrt{\phi} I(Q), \quad (4)$$

where $\phi \in [0, 1]$ is the fraction of the total metaorder volume that has been executed. $\phi = 0$ at the start of the metaorder and $\phi = 1$ by the end of the metaorder. More concretely, $\phi = \sum_{i=1}^n q_i / Q$ and q_i is the volume traded in a single child order of a metaorder of volume Q [14].

Since all the metaorders have different durations, we use ϕ as a volume based measure of time. This has the desired effect of standardising the duration to a unit long window $([0, 1])$. We also scale the price impact by $1/\sigma_D \sqrt{Q}$ to normalise the impact. Doing this changes the theoretical price impact profile to:

$$\frac{I(\phi \times Q)}{\sigma_D \sqrt{Q}} = \sqrt{\phi} \times \frac{I(Q)}{\sigma_D \sqrt{Q}} \quad (5)$$

We measured the impact profile of a metaorder as:

$$I(\phi \times Q) = \epsilon \times (\ln(m_{i+1}) - \ln(m_0)) \quad (6)$$

where m_0 is the mid-price just before the metaorder begins and m_{i+1} is the mid-price just after execution of the i^{th} child order. This is measured for each child order in a metaorder.

Figure 3 shows the impact profile during execution of the metaorders for GFI and GRT with the fitted curve of the profile shown in red. Metaorders were generated by

Description	Ticker	$\gamma_1 [\times 10^{-4}]$	γ_2
Gold Fields Ltd.	GFI	9.79 ± 0.20	1.001 ± 0.044
Growthpoint Ltd.	GRT	4.54 ± 0.14	0.766 ± 0.057

Table 1: Fitted values for metaorder execution profiles of GFI and GRT for the scaling factor γ_1 , and the exponent γ_2 from Equation 7. These are the fits for Figure 3a for GFI and Figure 3b for GRT.

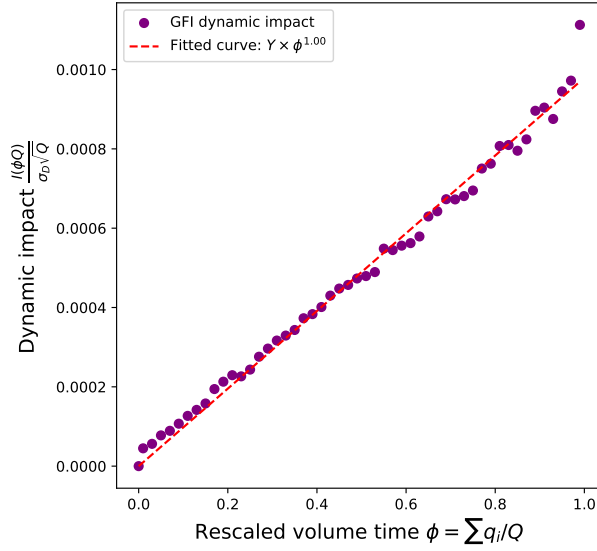
specifying 20 traders and a power-law trader participation distribution with $\delta = 2$. Only metaorders with 10 or more child orders were used for this analysis. It was assumed that:

$$\frac{I(\phi \times Q)}{\sigma_D \sqrt{Q}} = \gamma_1 \times \phi^{\gamma_2}. \quad (7)$$

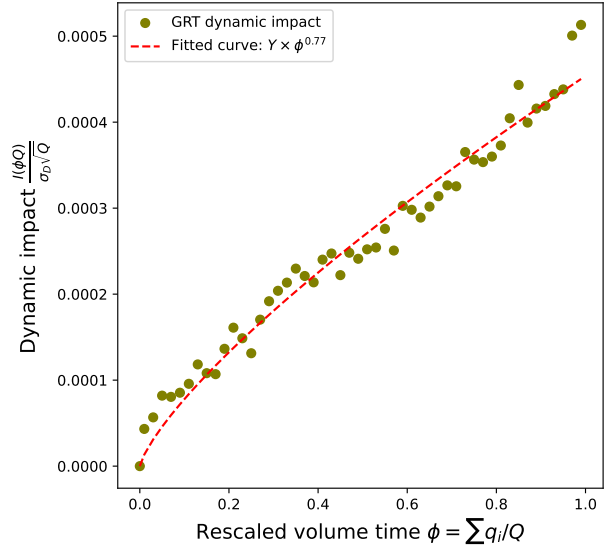
Here ϕ is still the fraction of the measured metaorder as in Equation 4. Numerical optimisation⁵ was used to estimate the values of $\gamma_{1,2}$. The values reported in Table 1 are point estimates with the 95% wald confidence interval half widths. The plots were made by binning ϕ and using the mean dynamic impact of each bin as the representative y value.

From Figure 3b and Table 1 we notice that for GRT the metaorders are on average with concave execution profiles. The parameter estimate of γ_2 for GRT is 0.77 ± 0.06 , indicating that there is indeed concavity in the execution profile. The concavity is however less than the theoretical, which proposed a γ_2 value of 0.5. Similarly, the parameter estimate of the scaling factor $\gamma_1 = 4.5 \pm 0.1 \times 10^{-4}$ which

⁵curve_fit was used for the optimisation, this uses non-linear least squares to fit a curve to the data.



(a) GFI



(b) GRT

Figure 3: Concave profile of metaorder impact. The dynamic impact is plotted as a function of ϕ , the proportion of the metaorder which has been executed, for (a) GFI (more liquid) and (b) GRT (less liquid). Metaorders were generated by specifying 20 traders and a power-law trader participation distribution with $\delta = 2$. Only metaorders with 10 or more child orders were used for this analysis. The fitted curves are shown in red. See Table 1 for the fitted profiles for GFI and GRT respectively using Equation 7.

is quite similar to the actual peak dynamic impact value near 5.0×10^{-4} . This matches the theory which proposed a scaling factor equal to the peak impact.

However, while the execution profile for GRT is concave, Figure 3b shows that the execution profile for GFI lacks the characteristic concavity that we expect from real metaorders. Table 1 indicates that the parameter estimate of γ_2 is approximately unity, which is linear. This result is likely due to an improper specification of the number of traders N and highlights the need for stock specific tuning when using this method of synthetic metaorder generation.

3.5. Post metaorder execution impact decay

Next, we investigate the convex decay of price impact after execution of the metaorder. Using the same theoretical impact decay function as [14]:

$$I(Q, z) = I(Q) \left(z^{1-\beta} - (z-1)^{1-\beta} \right) \quad (8)$$

and scaling by $1/\sigma_D \sqrt{Q}$, we get a new theoretical decay function:

$$\frac{I(Q, z)}{\sigma_D \sqrt{Q}} = \frac{I(Q)}{\sigma_D \sqrt{Q}} \times \left(z^{1-\beta} - (z-1)^{1-\beta} \right) \quad (9)$$

where $z = \frac{t}{T} \geq 1$ is rescaled time. t is the time since the start of the metaorder *i.e.*, $t = 0$ corresponds to the start of the metaorder, $t = T$ corresponds to the end of the metaorder and $t > T$ is after the metaorder. T is once

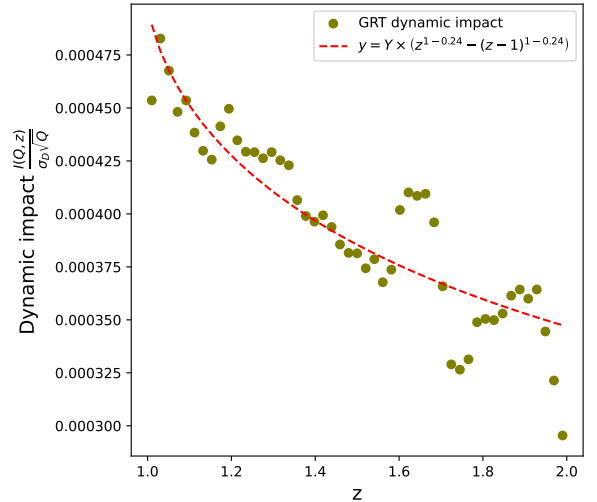


Figure 4: Convex post execution decay of impact for GRT. Dynamic impact is plotted as a function of z , the rescaled time. Metaorders were generated by specifying 20 traders and a power-law trader participation distribution with $\delta = 2$. The fitted line is shown in red.

again the duration of the metaorder. Both t and T were measured in minutes.

Figure 4 shows the observed impact decay for metaorders generated from GRT. The metaorders were once again generated by specifying 20 traders, a power-law trader participation distribution with $\delta = 2$ and only including

Description	Ticker	$\gamma_0 [\times 10^{-4}]$	β
Growthpoint Ltd.	GRT	5.01 ± 0.194	0.241 ± 0.033

Table 2: Fitted values for metaorder post execution impact decay for GRT.

metaorders with 10 or more child orders. The plot was produced by binning z values and using the mean dynamic impact of each bin as the representative y value.

From the Figure, it is clear that there is more noise compared to the execution profile (Figure 3b). However, assuming a relation of the form:

$$\frac{I(Q, z)}{\sigma_D \sqrt{Q}} = \gamma_0 \times (z^{1-\beta} - (z-1)^{1-\beta}) \quad (10)$$

we were still able to find estimates of the prefactor δ and for β . Table 2 reports the point estimates along with the half widths of a 95% wald confidence interval. The estimated value for β was found to be 0.241. This result closely matches the result of $\beta = 0.19$ obtained in [14] which used synthetic metaorders, and matches even more closely to the $\beta = 0.22$ result obtained in [4] which used real metaorders. We also recovered a $\gamma_0 = 5.01 \pm 0.2 \times 10^{-4}$ which matches the observed peak dynamic impact near 5×10^{-4} . This result is accordance with the theory which suggests a prefactor of $\frac{I(Q)}{\sigma_D \sqrt{Q}}$. Check Equation 9.

3.6. Validation of the synthetic metaorders

We have shown that the synthetic metaorders we have generated do indeed reproduce the key stylised facts of metaorders, namely, the square-root law, time independence of impact, concave execution profile and the convex impact decay. This suggests that algorithm 1 and 2 capture the dynamics of market activity and as such, allow us to use these synthetic metaorders to investigate the LMF theory.

3.7. Example metaorder execution profile

Figure 3b shows the execution profile of all metaorders with 10 or more child orders when specifying 20 traders and a power-law trader participation distribution with $\delta = 2$ for GRT. Table 1 reports the fitted values of a curve of the form $\gamma_1 \times \phi^{\gamma_2}$ for both GRT and GFI. Specifically, γ_2 for GRT was found to be 0.77 ± 0.06 . It is therefore clear that, on average, the concavity of the execution profiles for GRT are much smaller than the theoretical, which suggests a γ_2 value of 0.5 (square-root)[14].

A likely reason for this mismatch is due to a misspecification in the number of traders N and the power-law exponent δ . Nevertheless, Table 3 and Figure 5 show the execution profile for a single metaorder from GRT when specifying 20 traders and a power-law trader distribution with $\delta = 2$.

Table 3 shows the value of ϕ , volume, mid price immediately after, and the impact profile of the individual

i	ϕ	m_{n+i}	$I(\phi \times Q) \times 10^{-4}$	Q
1	0.03	1478.00	6.77	2500.00
2	0.22	1479.00	13.53	14559.00
3	0.37	1479.00	13.53	11652.00
4	0.38	1479.50	16.91	989.00
5	0.39	1479.50	16.91	254.00
6	0.50	1479.50	16.91	8700.00
7	0.53	1479.50	16.91	2266.00
8	0.56	1480.00	20.29	2100.00
9	0.65	1479.50	16.91	7455.00
10	0.83	1480.00	20.29	13724.00
11	1.00	1479.50	16.91	13181.00

Table 3: Example metaorder from GRT with 20 traders and a power-law trader participation distribution

child orders (check Equation 6 for details on how the impact profile was calculated.) of the metaorder. Figure 5 shows the execution profiles when using the peak impact $I(Q)$ and when using the peak dynamic impact $\frac{I(Q)}{\sigma_D \sqrt{Q}}$. The actual observed execution profile, while not perfectly aligned with the theoretical curve, does exhibit a similar level of concavity. This shows that there are metaorders which match the theoretical execution profile, but due to misspecification of the number of traders, the aggregate execution profile is flattened.

4. Testing the LMF theory

The Lillo-Mike-Farmer (LMF) theory provides a microscopic explanation for the long-range correlation (LRC) observed in market-order flow. Empirically, trade signs of market orders exhibit strong persistence. Specifically, autocorrelations in trade signs have a power-law decay in time-lag τ . To show this, we start by first defining the autocorrelation as:

$$\hat{C}(\tau) := \sum_{\ell=1}^{N_\epsilon - \tau} \frac{\epsilon_\ell \epsilon_{\ell+\tau}}{N_\epsilon - \tau}, \quad (11)$$

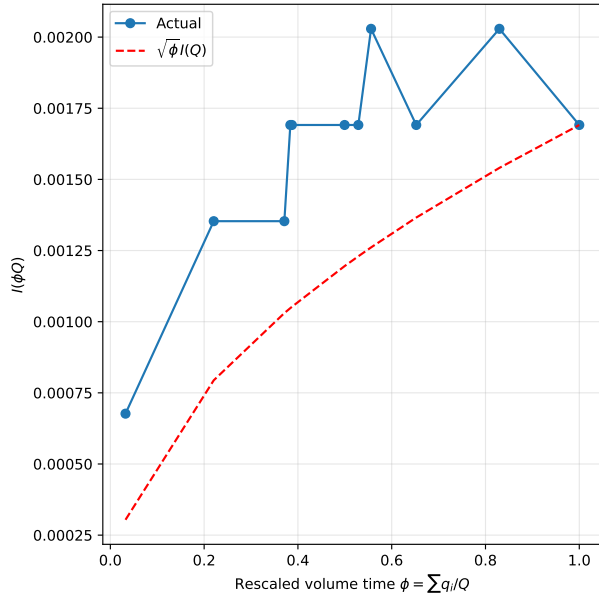
where $\epsilon_\ell = \pm 1$ are the measured market order signs, N_ϵ is the number of market orders. The LMF model attributes this macroscopic long memory to the microscopic behavior of order-splitting traders (STs) who divide large metaorders into sequences of smaller child orders of the same sign [16].

4.1. Relationship between γ and α

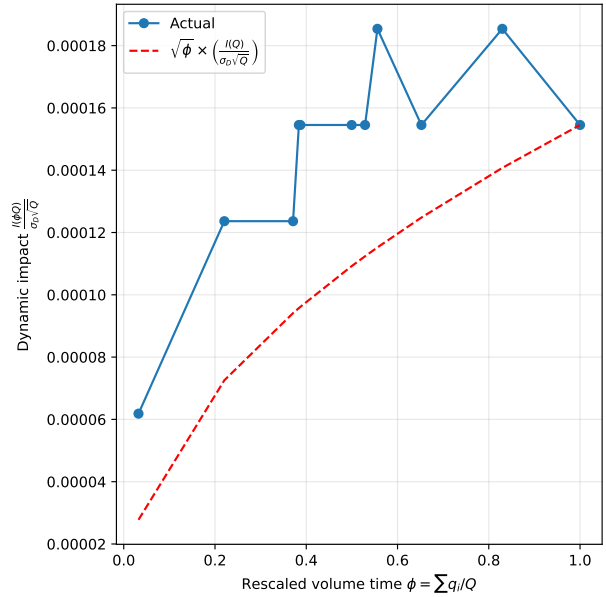
The key assumption of the LMF model is that metaorder lengths L follow a power-law distribution:

$$P(L) \sim L^{-\alpha-1}, \quad \alpha > 1, \quad (12)$$

and that the presence of STs is sufficient to generate the observed LRC. Under the assumption of random order



(a) Peak impact



(b) Peak dynamic impact

Figure 5: The execution profiles of a single metaorder from GRT when using (a), the peak impact $I(Q)$ and (b), when using the peak dynamic impact. Metaorders were generated by specifying 20 traders and a power-law trader participation distribution. The theoretical profiles are shown in red.

submissions by STs, the model predicts a simple quantitative relation between the microscopic exponent α and the macroscopic LRC exponent γ :

$$\gamma = \alpha - 1. \quad (13)$$

This remarkable result connects a directly measurable macroscopic property of the market (the decay of order autocorrelations) to a microscopic property of trader behaviour (the distribution of metaorder sizes).

4.2. Empirical Estimation of α and γ

To test this prediction, we first classify traders into STs and random traders (RTs) using a strategy clustering procedure. Metaorder lengths L are then extracted as consecutive sequences of same-sign orders from STs. Using the [Clauset et al.](#) method for power-law fitting, we estimate the exponent α for each stock in our dataset [16]. Simultaneously, we compute the autocorrelation function of the market order signs and fit the decay to estimate γ using an unbiased estimator that corrects for finite-sample bias.

Figure 6 shows the empirical relationship between α and γ for two sample scenarios: 50 traders with a power-law distribution of trading intensity and $\delta = 2$ (Figure 6a) and 150 traders with power-law distribution of trading intensity with $\delta = 2$ (Figure 6b). The median of each bin is indicated in orange. As predicted by the LMF theory, the data points lie close to the line $\gamma = \alpha - 1$, confirming that the long-range correlation of order signs is quantitatively explained by the distribution of metaorder lengths.

5. Conclusion

In Section 3 we have shown that we are able to generate synthetic metaorders from public TAQ data using the methods proposed by Maitrier et al. [14]. Figure 1 shows that the impact of the synthetic metaorders obey the square root law. In particular, Figure 1b shows that the aggregated metaorder impact of all the stocks in the top 100 show remarkable obedience to the theoretical square root law. Figure 2 shows that the impact of the synthetic metaorders are independent of their durations. Figure 3 shows that the execution profile of the synthetic metaorders is concave, indicating that the impact is not linear in ϕ . The impact is large initially, but tapers down as the metaorder nears completion. Figure 4 shows that post execution, the impact is non permanent and decays according to Equation 9. Together, these figures show that the synthetic metaorders are indeed realistic.

In Section 4 we show that using the synthetic metaorders, we can recover the approximate relation $\gamma = \alpha - 1$ that is proposed in [13]. Figure 6 shows the approximate relation we recover when using a power-law distribution with 50 traders (Figure 6a) and when using a power-law distribution with 150 trades (Figure 6b). These results are consistent with the results obtained by Sato and Kanazawa [16] in which real metaorder data was used.

These results show that we can recover realistic synthetic metaorders from public TAQ data and then use those synthetic metaorders to show that there is a relationship between the long range correlation decay exponent γ , and the power-law exponent α , of the metaorder

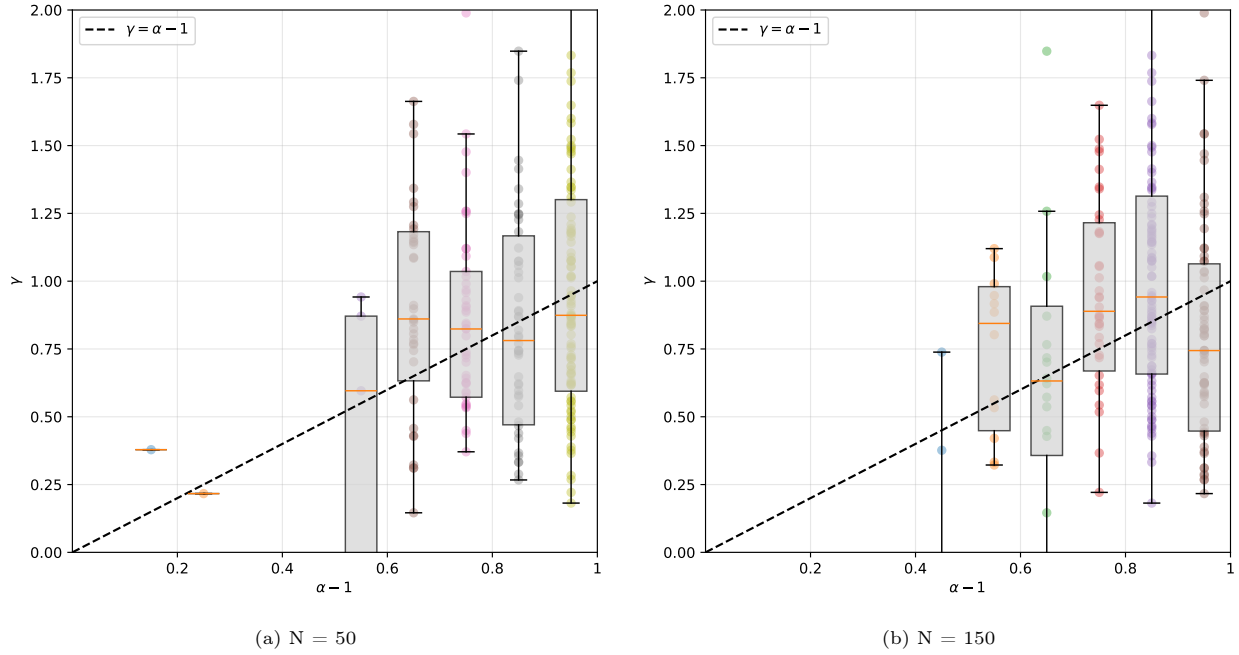


Figure 6: Scattered box plots between $\alpha - 1$ and γ with the median indicated in orange. (a) shows the results when using 50 traders with power-law trader distribution and (b) shows the result when using 150 traders with a power-law distribution. In both cases, $\delta = 2$.

run lengths distribution.

The results are consistent with related agent-based modelling work where the metaorders were modelled as learnt TWAP strategies executed by multiple interacting reinforcement learning agents [7], and then aggregated in a reactive agent-based model [8] (in particular their Figure 6). They demonstrate how the decay in the trade sign autocorrelations caused by metaorders mixing with other agents can be tuned to fit the empirical data while retaining little memory in the price fluctuations, and recover a square root price impact law and hence the required convexity in the price impact of orders.

This can then be shown to be consistent and recoverable using reaction-diffusion simulation methods [6] following the latent order-book approach of Mastromatteo et al. [15], Donier et al. [9]. This both validates the centrality of metaorder flow in the generation of long-memory in financial markets, but also demonstrates what is necessary (and sufficient) for reasonably realistic simulations of financial markets beyond the sequential time and low-frequency regime typical of most older agent-based models.

6. Acknowledgements

We would like to thank Nasheen Sharma and Vuyo Mashiqqa from the JSE, and the JSE for supporting the project. We thank Daniela Stevenson for suggestions and feedback.

References

- [1] Bacry, E., Iuga, A., Lasnier, M., Lehalle, C.A., 2014. Market impacts and the life cycle of investors orders. URL: <https://arxiv.org/abs/1412.0217>, arXiv:1412.0217.
- [2] BMLL Technologies, 2026. BMLL Data Lab Python Development Environment. URL: <https://www.bmlitech.com/>. accessed: 2026-02-02.
- [3] Bouchaud, J.P., 2025. The universal law behind market price swings. *Physics* 18, 196. URL: <https://physics.aps.org/articles/v18/196>.
- [4] Brokmann, X., Serie, E., Kockelkoren, J., Bouchaud, J.P., 2014. Slow decay of impact in equity markets. URL: <https://arxiv.org/abs/1407.3390>, arXiv:1407.3390.
- [5] Clauset, A., Shalizi, C.R., Newman, M.E.J., 2009. Power-law distributions in empirical data. *SIAM Review* 51, 661–703. URL: <http://dx.doi.org/10.1137/070710111>, doi:10.1137/070710111.
- [6] Diana, D., Gebbie, T., 2025. Non-uniformly sampled simulated price impact of an order-book. *Journal of Computational and Applied Mathematics* 456, 116202. URL: <https://www.sciencedirect.com/science/article/pii/S0377042724004515>, doi:<https://doi.org/10.1016/j.cam.2024.116202>.
- [7] Dicks, M., Paskaramoorthy, A., Gebbie, T., 2023a. Many learning agents interacting with

- an agent-based market model. arXiv preprint arXiv:2303.07393 URL: <https://arxiv.org/abs/2303.07393>, arXiv:2303.07393.
- [8] Dicks, M., Paskaramoorthy, A., Gebbie, T., 2023b. A simple learning agent interacting with an agent-based market model. *Physica A: Statistical Mechanics and its Applications* URL: <https://doi.org/10.1016/j.physa.2023.129363>, doi:10.1016/j.physa.2023.129363.
- [9] Donier, J., Bonart, J., Mastromatteo, I., Bouchaud, J.P., 2015. A fully consistent, minimal model for non-linear market impact. *Quantitative Finance* 15, 1109–1121. URL: <https://doi.org/10.1080/14697688.2015.1032540>, doi:10.1080/14697688.2015.1032540.
- [10] Goliath, E., Gebbie, T., 2026. Metaorder modelling and identification (github repository). <https://github.com/EzraGoliath/Metaorder-modelling-and-identification-Msc-thesis> Accessed: 2026-02-17.
- [11] Lillo, F., 2023. Decoding the dynamics of supply and demand. *Physics* 16, 192. URL: <https://physics.aps.org/articles/v16/192>.
- [12] Lillo, F., Farmer, J.D., 2004. The long memory of the efficient market. *Studies in Nonlinear Dynamics and Econometrics* 8. doi:10.2202/1558-3708.1144.
- [13] Lillo, F., Mike, S., Farmer, J.D., 2005. Theory for long memory in supply and demand. *Phys. Rev. E* 71, 066122. URL: <https://link.aps.org/doi/10.1103/PhysRevE.71.066122>, doi:10.1103/PhysRevE.71.066122.
- [14] Maitrier, G., Loeper, G., Bouchaud, J.P., 2025. Generating realistic metaorders from public data. URL: <https://arxiv.org/abs/2503.18199>, arXiv:2503.18199.
- [15] Mastromatteo, I., Toth, B., Bouchaud, J.P., 2014. Agent-based models for latent liquidity and concave price impact. *Physical Review E* 89, 042805. URL: <https://doi.org/10.1103/PhysRevE.89.042805>, doi:10.1103/PhysRevE.89.042805.
- [16] Sato, Y., Kanazawa, K., 2023a. Inferring microscopic financial information from the long memory in market-order flow: A quantitative test of the lillo-mike-farmer model. *Physical Review Letters* 131, 197401. URL: <https://link.aps.org/doi/10.1103/PhysRevLett.131.197401>, doi:10.1103/PhysRevLett.131.197401.
- [17] Sato, Y., Kanazawa, K., 2023b. Quantitative statistical analysis of order-splitting behavior of individual trading accounts in the Japanese stock market over nine years. *Physical Review Research* 5, 043131. URL: <https://link.aps.org/doi/10.1103/PhysRevResearch.5.043131>, doi:10.1103/PhysRevResearch.5.043131.
- [18] Tóth, B., Eisler, Z., Lillo, F., Kockelkoren, J., Bouchaud, J.P., 2011. How does the market use information? evidence from the response of prices to trades. *Quantitative Finance* 11, 817–828. doi:10.1080/14697688.2010.481632.
- [19] Tóth, B., Lempérière, Y., Deremble, C., de Lataillade, J., Kockelkoren, J., Bouchaud, J.P., 2011. Anomalous price impact and the critical nature of liquidity in financial markets. *Physical Review X* 1. URL: <http://dx.doi.org/10.1103/PhysRevX.1.021006>, doi:10.1103/physrevx.1.021006.
- [20] Wilcox, D., Gebbie, T., 2014. Hierarchical causality in financial economics. arXiv preprint arXiv:1408.5585 doi:10.48550/arXiv.1408.5585.

7. Appendix

7.1. Stocks used in the analysis

The 100 stocks used in the analyses are shown in Table 4. The table displays the tickers as presented by the JSE. These specific stocks were selected by sorting all the stocks on the JSE by volume traded and then choosing the first 100 that contained data from 1 Jan 2023 to 31 Dec 2025.

7.2. Sample of the processed data

Table 5 reports a snippet of the raw data after some basic processing. The data from BMLL [2] was cleaned and had some basic processing done to it. The only processing done by us was the addition of the Mid-price after (delayed), the Daily Volume, Daily volatility and Daily Volatility (alt). *Mid-price after (delayed)* is mid-price after the trade and just before the following trade. These values were not used in the analyses, only *Mid-price after (immediate)* was used in the analyses. *Daily Volume* is the total volume executed in the day. *Daily volatility* is the daily volatility, calculated as in Algorithm 2. *Daily Volatility (alt)* is an alternate way of calculating the daily volatility but calculated as $\ln(m_{\max}) - \ln(m_{\min})$. These values were never used in the analyses.

7.3. Sample of data after applying algorithms 1 and 2

Table 6 shows a snippet of the processed data after applying algorithms 1 and 2. We generated the synthetic metaorders by specifying 4 traders and a homogeneous trader participation distribution. The table shows the first 5 metaorders for Anglo American plc (Ticker AGL).

ABG	ACL	AEG	AEL
AFE	AFT	AGL	ANG
ANH	APN	ARI	AVI
BHG	BID	BLU	BOX
BTI	BTN	BVT	BYI
CCD	CLS	CML	CPR
DCP	DIB	DRD	DSY
EQU	EXX	FFB	FSR
FTB	GFI	GLN	GND
GRT	HAR	IMP	INL
INP	ITE	JBL	KAP
KP2	KST	LAB	LHC
LTE	MDI	MNP	MRP
MSP	MTM	MTN	N91
NED	NPH	NPN	NRP
NTC	NY1	OMN	OMU
OPA	ORN	OUT	PAN
PIK	PPC	PPE	PPH
PRX	QLT	RBO	RDF
REM	RNI	S32	SAC
SAP	SBK	SHP	SLM
SOL	SPG	SRE	SSS
SSU	SSW	TFG	TGA
TKG	TRU	VAL	VKE
VOD	WBC	WHL	YRK

Table 4: The JSE tickers of the 100 stocks used in the analyses for the project. [2][2] ticker names and descriptions and listing dates corporate actions references. See Table 5 for an example of the panel of processed data (after the data engineering) that is ready for the datascience.

The table reports multiple different versions of *impact* but only *impact(simple)* was used in the analyses. For convenience we have referred to *impact(simple)* as just the *impact*.

Panel A

Row	MIC	Ticker	ListingId	Date	DateTime	ExchangeSequenceNumber	Daily Volume	Daily Volatility
1	XJSE	AGL	418405540	2023-01-03	2023-01-03 09:01:34.362134	74722	453236.000000	0.018747
2	XJSE	AGL	418405540	2023-01-03	2023-01-03 09:01:34.362332	74724	453236.000000	0.018747
3	XJSE	AGL	418405540	2023-01-03	2023-01-03 09:01:58.046172	86046	453236.000000	0.018747
4	XJSE	AGL	418405540	2023-01-03	2023-01-03 09:01:58.296837	86214	453236.000000	0.018747
5	XJSE	AGL	418405540	2023-01-03	2023-01-03 09:03:21.577601	111646	453236.000000	0.018747

Panel B

Row	Trade Sign	Trade Price	Volume	Mid-price before	Mid-price after(immediate)	Mid-price after(delayed)	Daily Volatility(alt)
1	1	66400.000000	8.000000	66258.500000	66259.000000	66258.500000	0.018674
2	1	66399.000000	5.000000	66258.500000	66259.000000	66213.000000	0.018674
3	1	66200.000000	1000.000000	66213.000000	66214.500000	66214.500000	0.018674
4	1	66164.000000	141.000000	66214.500000	66215.500000	66227.500000	0.018674
5	1	66298.000000	1.000000	66227.500000	66227.500000	66262.500000	0.018674

Table 5: Sample of processed data for Anglo American plc (Ticker AGL)

Table 6: Sample of processed data for Anglo American plc (Ticker AGL) after applying algorithms 1 and 2

Panel A										
Row	RIC	Date	Start time	End time	daily volume	intraday volatility	number child orders	volume traded		
1	AGL	2023-01-03	2023-01-03 09:05:07.210790	2023-01-03 09:15:38.527148	453236.000000	0.018747	4	418.000000		
2	AGL	2023-01-03	2023-01-03 09:18:48.526544	2023-01-03 09:23:20.103792	453236.000000	0.018747	6	324.000000		
3	AGL	2023-01-03	2023-01-03 09:24:17.372554	2023-01-03 09:24:42.540623	453236.000000	0.018747	3	291.000000		
4	AGL	2023-01-03	2023-01-03 09:25:00.119142	2023-01-03 09:28:31.092101	453236.000000	0.018747	5	425.000000		
5	AGL	2023-01-03	2023-01-03 09:35:12.840937	2023-01-03 09:35:23.140791	453236.000000	0.018747	4	231.000000		

Panel B										
Row	trade sign	impact(shortfall)	impact(ave per trade)	impact(simple)	20 AD volume	20 AD volatility				
1	1	0.002170	0.000258	0.006093	453236.000000	0.018747				
2	-1	0.002989	0.000047	0.002456	453236.000000	0.018747				
3	1	0.000776	0.000493	0.000722	453236.000000	0.018747				
4	-1	0.002236	0.000047	0.002948	453236.000000	0.018747				
5	1	0.000723	0.000178	0.000686	453236.000000	0.018747				